Proportional Fair Coding for Wireless Mesh Networks

Karumbu Premkumar, *Member, IEEE*, Xiaomin Chen, and Douglas J. Leith, *Senior Member, IEEE*

***Abstract*—We consider multihop wireless networks carrying unicast flows for multiple users. Each flow has a specified delay deadline, and the lossy wireless links are modeled as binary symmetric channels (BSCs). Since transmission time, also called airtime, on the links is shared among flows, increasing the airtime for one flow comes at the cost of reducing the airtime available to other flows sharing the same link. We derive the joint allocation of flow airtimes and coding rates that achieves the proportionally fair throughput allocation. This utility optimization problem is nonconvex, and one of the technical contributions of this paper is to show that the proportional fair utility optimization can nevertheless be decomposed into a sequence of convex optimization problems. The solution to this sequence of convex problems is the unique solution to the original nonconvex optimization. Surprisingly, this solution can be written in an explicit form that yields considerable insight into the nature of the proportional fair joint airtime/coding rate allocation. To our knowledge, this is the first time that the utility fair joint allocation of airtime/coding rate has been analyzed, and also one of the first times that utility fairness with delay deadlines has been considered.**

***Index Terms*—Binary symmetric channels, code rate selection, cross-layer optimization, network utility maximization, optimal packet size, resource allocation, scheduling.**

I. Introduction

In this paper, we consider wireless mesh networks with lossy links and flow delay deadlines. Packets that are decoded after a delay deadline are treated as losses. We derive the joint allocation of flow airtimes and coding rates that achieves the proportionally fair throughput allocation. To our knowledge, this is the first time that the utility fair joint allocation of airtime/coding rate has been analyzed, and also one of the first times that utility fairness with delay deadlines has been considered (also, see [1] and [2]).

In the special cases where all links in a network are loss-free or all flow delay deadlines are infinite, we show that the proportionally fair utility optimization decomposes into decoupled airtime and coding rate allocation tasks. That is, a layered approach that separates MAC scheduling and packet coding rate selection is optimal. This corresponds to the current practice, and these tasks can be solved separately using a wealth of classical techniques.

Manuscript received November 26, 2012; revised June 15, 2013; accepted December 08, 2013; approved by IEEE/ACM Transactions on Networking Editor A. Proutiere. Date of publication January 28, 2014; date of current version February 12, 2015. This work was supported by the Science Foundation Ireland under Grants 07/IN.1/I901 and 11/PI/1177.

K. Premkumar was with the Hamilton Institute, NUI Maynooth, Maynooth, Ireland. He is now with the Department of Information Technology, SSN College of Engineering, Chennai 603 110, India (e-mail: kprem@ece.iisc.ernet.in).

X. Chen and D. J. Leith are with the Hamilton Institute, NUI Maynooth, Maynooth, Ireland (e-mail: Xiaomin.Chen@nuim.ie; Doug.Leith@nuim.ie).

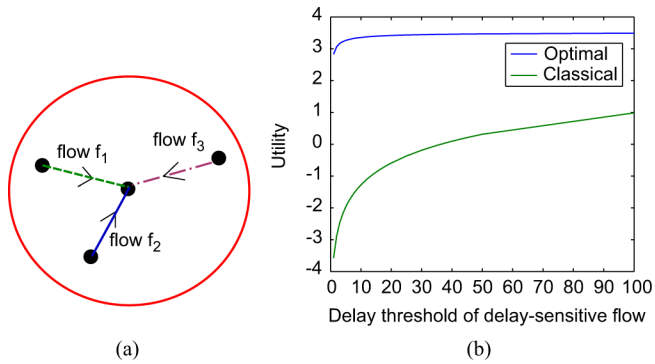

Fig. 1. Single-cell wireless LAN with three flows. The central node represents the access point (AP), and the other nodes represent the wireless stations. (a) Topology. (b) Optimum utility versus classical utility.

However, we show that no such decomposition occurs when one or more links are lossy or one or more flows have finite delay deadlines. Instead, in such cases, it is necessary to jointly optimize the flow airtimes and coding rates. Furthermore, we show that the resulting allocation of airtime and coding rates is qualitatively different from classical results. For example, consider a single-hop wireless network carrying three flows; see Fig. 1. Flow f_1 is a delay-sensitive flow (e.g., video), while flows f_2 and f_3 are delay-insensitive flows (e.g., TCP data). Transmissions are scheduled in a TDMA manner, and the delay deadline for flow f_1 is one schedule period, while the delay deadline for flows f_2 and f_3 is infinite. The channel symbol error rate is 10^{-2} for all flows, and flows use MDS codes for error correction. The proportionally fair airtime and coding rate allocation that we show in this paper [see (21) and (22)] results in the allocation of 41% of the airtime for flow f_1, while flow f_2 and flow f_3 each receive 29.5%. Observe that the proportionally fair allocation assigns unequal airtimes to the flows, which is a notable departure from the usual equal-airtime property of the proportional fair allocation when selection of delay deadlines and coding rate are not included, e.g., see [3]. The optimal coding rate is 0.62 for flow f_1 and 0.97 for flows f_2 and f_3. The coding rate for flow f_1 is much lower than for flows f_2 and f_3 since a smaller block size must be used by flow f_1 (and more redundant symbols for error recovery) in order to respect the delay deadline. Due to the delay deadline, these optimal coding rates yield nonzero loss rates. For flow f_1, the packet loss rate at the receiver, after decoding, is 20%, whereas flows f_2 and f_3 are loss-free. This highlights an important feature of the joint airtime and coding rate utility optimization. Namely, that it allows the throughput/loss/delay tradeoff among flows sharing network resources to be performed in a principled, fair

manner. Without consideration of coding rate, the tradeoff between throughput and loss cannot be fully understood or optimally managed. Without consideration of airtime, the contention between flows for shared network resources cannot be fully captured.

Proportional fairness can be formulated as a utility maximization task, with the utility being the sum of log flow rates. Fig. 1(b) compares the optimal network utility to that obtained with a classical type of approach where all flows are allocated equal airtime and the coding rates are chosen based on the channel error probabilities alone (this corresponds to ignoring the delay deadline of flow f_1). It can be seen that the optimal approach that we present in this paper potentially offers significant performance benefits over classical methods.

We note that one of the reasons why the joint selection of airtime/coding rate has not been previously studied is that the proportional fair utility optimization is nonconvex, and hence, powerful tools from convex optimization cannot be applied directly. Also, the study of the throughput performance by jointly considering the coding and the MAC has not been performed before. One of the technical contributions of this paper is to show that the proportional fair utility optimization can nevertheless be decomposed into a sequence of convex optimization problems. The solution to this sequence of convex problems is the unique solution to the original nonconvex optimization. Moreover, this solution can be written in an explicit form thereby yielding considerable insight into the nature of the proportional fair airtime/coding rate allocation.

Our analysis encompasses both hop-by-hop FEC and end-to-end FEC and hybrid combinations of these. For example, hop-by-hop FEC can be accommodated by partitioning an end-to-end route into segments and applying our results to each segment individually (a segment here might consist of a single hop or, more generally, several hops). Our analysis is also relevant to the use of corrupted frames as an information channel. Recent measurement studies find that the number of erroneous bits in corrupted frames is often rather small, and so these frames potentially provide a useful information channel (e.g., [4] suggests potential capacity gains of 100% might be achieved in this way). In this case, there already exists hop-by-hop FEC at the PHY/MAC layer, and the end-to-end FEC is concatenated with this. Since the hop-by-hop PHY/MAC FEC is typically strongly constrained by the link hardware (e.g., it cannot exploit recent improvements in code efficiency nor take account of flow-level requirements), the addition of coding above the link layer can yield extra performance.

The rest of the paper is organized as follows. The related literature on utility optimal resource allocation is discussed in Section II. Section III defines the network model; in particular, we describe the mesh network architecture, the traffic model, and the channel model. We also discuss the transmission scheduling model, decoding delay deadline, and the network constraints. In Section IV, we obtain a measure for the end-to-end packet decoding error and describe the throughput of the network. In Section V, we formulate a network utility maximization problem subject to constraints on the transmission schedule lengths and discuss the optimization framework. In Section VI, we discuss two special cases of networks, delay-insensitive and loss-free networks, and show that the tasks of obtaining optimal airtimes and coding rates decouple in these special cases. We discuss the optimal airtime/coding solution with some examples in Section VII. Finally, we conclude in Section VIII. The proofs of lemmas and theorems are provided in the Appendix.

II. Related Work

We consider a multihop Network Utility Maximization (NUM) problem with deadline constraints and with a practical model [4] for the PHY layer. By means of channel coding, we try to recover a packet from the channel errors. Having a low coding rate helps in recovering the packets, but at the cost of a small fraction of payload and at the cost of the transmission airtime of other flows. Thus, we consider the problem of resource allocation that answers the following question: *how to allocate throughput across competing flows with each flow seeing different channel conditions and respecting the delay deadline.*

The problem of NUM has been studied in various contexts, with NUM as a network layering tool introduced in [5].

Much of the work on NUM is concerned with the flow scheduling and throughput allocation that achieves the network stability region. This work focuses on throughput and largely ignores delay constraints. Resource allocation problems from the viewpoint of network control and stability is studied by Georgiadis *et al.* in [6]. Network flow scheduling problems are studied in a utility optimal framework by Shakkottai and Srikant in [7]. In all these works and the references therein, the emphasis is on the MAC layers and above. In [6], an energy optimal scheduling problem is studied in which the PHYsical layer is also considered.

Some recent work explicitly includes delay constraints in the utility optimization. In [1], Li and Eryilmaz studied the problem of end-to-end delay constrained scheduling in multihop networks. They propose algorithms based on Lyapunov drift minimization and pricing, and show that by dynamically selecting service disciplines, the proposed algorithms significantly outperform existing throughput-optimal scheduling algorithms. In [2], Jaramillo and Srikant studied a resource allocation problem in ad hoc networks with elastic and inelastic traffic with deadlines for packet reception, and obtained joint congestion control and scheduling algorithm that maximizes a network utility. In [2], the focus is on congestion control and scheduling, with the PHYsical layer considered to be error-free.

A short, preliminary version of the work in the current paper was presented in [8].

III. Network Model

A. Cellular Mesh Architecture

We consider networks consisting of a set of $C \geq 1$ cells, $\mathcal{C} = \{1, 2, \ldots, C\}$, which define the "interference domains" in the network. We allow intracell interference (i.e., transmissions by nodes within the same cell interfere), but assume that there is no intercell interference. This captures, for example, common network architectures where nodes within a given cell

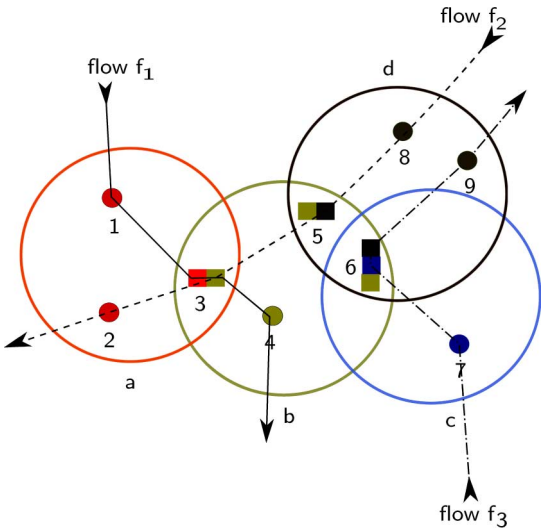

Fig. 2. Wireless mesh network with four cells. Cells a, b, c, and d use orthogonal channels CH_1, CH_2, CH_3, and CH_4, respectively. Nodes 3, 5, and 6 are *bridge nodes*. The bridge node 3 (resp. 5 and 6) is provided a time slice of each of the channels CH_1 and CH_2 (resp. CH_2 and CH_4 for node 5, and CH_2, CH_3, and CH_4 for node 6). Three flows f_1, f_2, and f_3 are considered. In this example, $\mathcal{C}_{f_1} = \{a, b\}$, $\mathcal{C}_{f_2} = \{d, b, a\}$, and $\mathcal{C}_{f_3} = \{c, d\}$.

use the same radio channel while neighboring cells use orthogonal radio channels. Within each cell, any two nodes are within the decoding range of each other and, hence, can communicate with each other. The cells are interconnected using multiradio bridging nodes to create a multihop wireless network. A multiradio bridging node i connecting the set of cells $\mathcal{B}(i) = \{c_1, .., c_n\} \subset \mathcal{C}$ can be thought of as a set of n single radio nodes, one in each cell, interconnected by a high-speed, loss-free wired backplane. See, for example, Fig. 2.

B. Unicast Flows

Data are transmitted across this multihop network as a set $\mathcal{F} = \{1, 2, \ldots, F\}$, $F \geq 1$ of unicast flows. The route of each flow $f \in \mathcal{F}$ is given by a sequence of cells $\mathcal{C}_f = \{c_1(f), c_2(f), \ldots, c_{\ell_f}(f)\}$, where the source node $s(f) \in c_1(f)$ and the destination node $d(f) \in c_{\ell_f}(f)$. We assume loop-free flows (i.e., no two cells in $\mathcal{C}_f$ are the same).

C. Binary Symmetric Channels

We associate a binary random variable $E_{f,c}[b]$ with the bth bit transmitted by flow f in cell c. $E_{f,c}[b] = 0$ indicates that the bit is received correctly, and $E_{f,c}[b] = 1$ indicates that the bit is received incorrectly, i.e., the bit is "flipped." We assume that $E_{f,c}[1], E_{f,c}[2], \ldots$ are independent and identically distributed (i.i.d.), and $\mathbb{P}\{E_{f,c}[b] = 1\} = \alpha_{f,c} \in [0, 0.5)$. That is, we have a binary symmetric channel (BSC) with crossover probability $\alpha_{f,c}$. A transmitted bit may be "flipped" multiple times as it travels along the route of flow f and is received incorrectly at the flow destination only if there is an odd number of such flips. The end-to-end crossover probability along the route of flow f is therefore given by

$$\alpha_f = \sum_{\{\chi_c \in \{0,1\}, c \in \mathcal{C}_f : \sum_{c \in \mathcal{C}_f} \chi_c \text{ is odd}\}} \prod_{c \in \mathcal{C}_f} \alpha_{f,c}^{\chi_c} \, (1 - \alpha_{f,c})^{1 - \chi_c}.$$

Note that we can accommodate transmission of symbols from any $2^m = M$-ary alphabet (i.e., not just transmission of binary symbols) by associating m channel uses of the BSC for every transmitted symbol. The symbol error probability (for any $m \geq 1$) is then given by $\beta_f = 1 - (1 - \alpha_f)^m$.

In this channel model, the channel processes across time are independent copies of the BSCs. In practice, this can be realized by means of an interleaver of sufficient depth (after the channel encoder), which randomly shuffles the encoded symbols subject to the delay deadline, combined with a de-interleaver (before the channel decoder) at the receiver. This interleaving and de-interleaving randomly mixes any channel fades, which can then be modeled as independent channel processes across time.

D. Flow Transmission Scheduling

A scheduler assigns a time slice of duration $T_{f,c} > 0$ s to each flow f that flows through cell c, subject to the constraint that $\sum_{f : c \in \mathcal{C}_f} T_{f,c} \leq T_c$ where T_c is the period of the schedule in cell c in seconds. We consider a periodic scheduling strategy in which, in each cell c, service is given to the flows in a round-robin fashion, and that each flow f in cell c gets a time slice of $T_{f,c}$ seconds in every schedule. We define *time-slot* corresponding to flow f in cell c as the time slice $T_{f,c}$ in each schedule length that serves the flow f.

E. Flow Decoding Delay Deadline

At the source node $s(f)$ for flow f, we assume that k_f symbols arrive in each schedule length $T_{c_1(f)}$, which allows us to simplify the analysis by ignoring queueing. Information symbols are formed into blocks of $D_f k_f$ symbols, where $D_f \in \{1, 2, 3, \ldots\}$ is the number of time-slots that the block may span. Each block of $D_f k_f$ information symbols is encoded into a block of $D_f n_f$ coded symbols, where $n_f = k_f / r_f$ symbols, with coding rate $0 < r_f \leq 1$. Here, n_f is the number of encoded symbols transmitted in one slot, i.e., the transmitted packet size. The code employed for encoding is discussed in Section IV. The quantity D_f is a user or operator supplied quality of service parameter. It specifies the decoding delay deadline for flow f, since after the flow destination has collected at most D_f successive coded packets, it must attempt to decode the encoded information symbols. Note that D_f also captures the encoding delay for nonsystematic codes—while systematic and convolutional codes incur no encoding delay at the transmitter, nonsystematic codes require the transmitter to wait for D_f symbols to be received before producing the first coded symbol.

The end-to-end delay deadline is given by the following: For the first chunk, the delay is $\sum_{c \in \mathcal{C}_f} T_c$, and for each of the remaining $D_f - 1$ chunks, the delay is $T_{d(f)}$ (recall that $d(f)$ is the destination cell of flow f). Thus, the end-to-end delay deadline is

$$\sum_{c \in \mathcal{C}_f} T_c + (D_f - 1) T_{d(f)}.$$

In the case of equal T_c's, the end-to-end delay deadline is

$$(\ell_f + D_f - 1) T_c$$

where we recall that ℓ_f is the number of links of flow f.

F. Network Constraints on Coding Rate

For flow f in cell c, let $w_{f,c}$ be the rate of transmission in symbols/second, which is determined by the modulation and spectral bandwidth used for signal transmission and the within-cell FEC used. Each cell $c \in \mathcal{C}_f$ along the route of flow f allocates an airtime of at least $\frac{n_f}{w_{f,c}}$ in order to transmit the packets of flow f. Let $\mathcal{F}_c := \{f \in \mathcal{F} : c \in \mathcal{C}_f\}$ be the set of flows that are routed through cell c. We recall that the transmissions in any cell c are scheduled in a TDMA fashion, and hence, the total time required for transmitting packets for all flows in cell c is given by $\sum_{f \in \mathcal{F}_c} \frac{n_f}{w_{f,c}}$. Since, for cell c, the transmission schedule interval is T_c units of time, the encoded packet size n_f must satisfy the schedulability constraint

$$\sum_{f \in \mathcal{F}_c} \frac{n_f}{w_{f,c}} \leqslant T_c.$$

Note that since we provide sufficient transmit time at each cell along route $\mathcal{C}_f$ to allow n_f coded symbols to be transmitted in every scheduled time-slot $T_{f,c}$, $c \in \mathcal{C}_f$, there is no queueing at the cells along the route of a flow.

IV. Packet Error Probability

Each transmitted symbol of flow f reaches the destination node erroneously with probability β_f. Hence, to help protect against errors when recovering the information symbols, we encode information symbols at the source nodes using a block code (we note here that a convolutional code with zero-padding is also a block code). An (n, k, d) block code has the following properties. The encoder takes a sequence of k information symbols as input and generates a sequence of $n \geq k$ coded symbols as output. The decoder takes a sequence of n coded symbols as input and outputs a sequence of k information symbols. These information symbols will be error-free provided no more than $\lfloor \frac{d-1}{2} \rfloor$ of the coded symbols are corrupted. The Singleton bound [9] tells us that $d \leqslant n - k + 1$, with equality for maximum-distance separable (MDS) codes. Thus, an MDS code can correct up to

$$\left\lfloor \frac{d-1}{2} \right\rfloor = \left\lfloor \frac{n-k}{2} \right\rfloor \tag{1}$$

errors. Examples for MDS codes include Reed–Solomon codes [9] and MDS-convolutional codes [10]. In [10], the authors show the existence of MDS-convolutional codes for any code rate. Hereafter, we will make use of (1), and so confine consideration to MDS codes. However, the analysis can be readily extended to other types of code provided a corresponding bound on d is available.

Consider a coded block of flow f and let $i \in \{1, 2, \ldots, D_f n_f\}$ index the symbols in the block. Let $E_f[i]$ be a binary random variable that equals 0 when the ith coded symbol is received correctly and that equals 1 when it is received corrupted. $\mathbb{P}\{E_f[i] = 1\} = \beta_f$, and $\mathbb{P}\{E_f[i] = 0\} = 1 - \beta_f$. From (1), the probability of the block being decoded incorrectly is given by

$$\widetilde{e}_f = \mathbb{P}\left\{ \sum_{i=1}^{D_f n_f} E_f[i] > \frac{D_f n_f - D_f k_f}{2} \right\}.$$

The symbol errors $E_f[1], E_f[2], \ldots, E_f[D_f n_f]$ are i.i.d. Bernoulli random variables, and so the $\sum_{i=1}^{D_f n_f} E_f[i]$ is a binomial random variable. Hence, the probability of a decoding error can be computed exactly. However, the exact expression is combinatorial in nature and is not tractable for further analysis. We therefore proceed by obtaining upper and lower bounds on the error probability and show that the bounds are the same up to a prefactor, and that the prefactor decreases as the block size $D_f n_f$ increases. Hence, we pose the NUM based on the upper bound on the error probability. Also, we relax the constraints $n_f \in \mathbb{Z}_+$ and $k_f \in \mathbb{Z}_+$ and allow them to take positive real values, i.e., $n_f \in \mathbb{R}_+$ and $k_f \in \mathbb{R}_+$.

A. Upper and Lower Bounds

Lemma 1: (Upper Bound). The end-to-end probability $\widetilde{e}_f$ of a decoding error for flow f satisfies

$$\begin{aligned} \widetilde{e}_f &\leq \exp\left(-D_f n_f I_{E_f[1]}(x_f; \theta_f)\right) \\ &=: e_f(\theta_f, n_f, x_f) \end{aligned} \tag{2}$$

where $x_f := \frac{1-r_f}{2}$, $r_f = k_f/n_f$ is the coding rate, $\theta_f > 0$ is the Chernoff-bound parameter, and the function $I_Z(x; \theta) := \theta x - \ln(\mathbb{E}\left[e^{\theta Z}\right])$ is called the rate function in large deviations theory.

Proof: See Appendix A. □

Lemma 2: (Lower Bound). The end-to-end probability $\widetilde{e}_f$ of a decoding error for flow f satisfies

$$\widetilde{e}_f \geq \Gamma \exp\left(-D_f n_f I\left(\mathcal{B}(x_f) \| \mathcal{B}(\beta_f)\right)\right) \tag{3}$$

where

$$\Gamma = \frac{\beta_f}{1-\beta_f} \exp\left(-D_f n_f H\left(\mathcal{B}(x_f)\right)\right)$$

and $x_f := \frac{1-r_f}{2}$, $\mathcal{B}(x)$ is the Bernoulli distribution with parameter x, and $H(\mathcal{P})$ is the entropy of probability mass function (pmf) $\mathcal{P}$.

Proof: See Appendix B. □

B. Tightness of Bounds

It can be verified that

$$I_{E_f[1]}(x_f; \theta_f) = \theta_f x_f - \ln\left(1 - \beta_f + \beta_f e^{\theta_f}\right).$$

Since $\theta_f > 0$ is a free parameter, we can select the value that maximizes $I_{E_f[1]}(x_f; \theta_f)$ and so provides the tightest upper bound. It can be verified (e.g., by inspection of the second derivative) that $I_{E_f[1]}(x_f; \theta_f)$ is concave in θ_f, and so the KKT conditions are necessary and sufficient for an optimum. The KKT condition here is

$$\left.\frac{\partial I_{E_f[1]}(x_f; \theta_f)}{\partial \theta_f}\right|_{\theta_f^*} = x_f - \left.\frac{\beta_f e^{\theta_f}}{1 - \beta_f + \beta_f e^{\theta_f}}\right|_{\theta_f^*} = 0$$

which is solved by

$$\theta_f^* = \ln\left(\frac{x_f}{\beta_f}\right) - \ln\left(\frac{1-x_f}{1-\beta_f}\right)$$

provided $x_f > \beta_f$. Substituting for θ_f^*

$$\begin{aligned}\max_{\theta_f>0} I_{E_f[1]}(x_f;\theta_f) &= I_{E_f[1]}\left(x_f;\theta_f^*\right)\\ &= x_f \ln\left(\frac{x_f}{\beta_f}\right) + (1-x_f)\ln\left(\frac{1-x_f}{1-\beta_f}\right)\\ &= I\left(\mathcal{B}(x_f)\,\|\mathcal{B}(\beta_f)\right)\end{aligned}$$

where $I(\mathcal{P}\|\mathcal{Q})$ is the information divergence between the pmfs $\mathcal{P}$ and $\mathcal{Q}$. Thus, by Lemmas 1 and 2 , the probability $\widetilde{e}_f$ of a decoding error satisfies

$$\Gamma e^{-D_f n_f I(\mathcal{B}(x_f)\|\mathcal{B}(\beta_f))} \le \widetilde{e}_f \le e^{-D_f n_f I(\mathcal{B}(x_f)\|\mathcal{B}(\beta_f))}.$$

It can be seen that the upper and lower bounds are the same to within prefactor Γ, and the gap between these bounds decreases exponentially as the block size $D_f n_f$ increases.

V. Network Utility Optimization

We are interested in the fair allocation of flow airtimes and coding rates among flows in the network. Other things being equal, we expect that decreasing the coding rate r_f (i.e., increasing the number $D_f n_f - D_f k_f$ of redundant symbols transmitted) for flow f will decrease the error probability e_f, and so increases the flow throughput. However, decreasing the coding rate increases the coded packet size $D_f n_f$, and so increases the airtime used by flow f. Since the network capacity is limited and shared by other flows, this generally decreases the airtime available to other flows, and so decreases their throughout. Similarly, increasing the packet size $D_f k_f$ of flow f increases its throughput, but at the cost of increased airtime and a reduction in the throughput of other flows. We formulate this tradeoff as a utility fair optimization problem. In particular, we focus on the proportional fair allocation since it is of wide interest and, as we will see, is tractable, despite the nonconvex nature of the optimization.

We consider a network utility function $U(\cdot)$ that is a function of the average network throughput. We recall that the arrival processes of symbols is such that for each flow f, k_f symbols arrive every $T_{c_1(f)}$ seconds, and hence, there is no queueing (i.e., there is no dynamics in the rate of transmission). However, the network throughput is stochastic due to the error process induced by the channel. Extending our work to include stochastic arrivals would be important and interesting. However, a queueing analysis with coupled queues seems likely to be intractable, so one possible strategy is to change to use of a fluid-like framework, although this would require a change in the definition of delay deadline used.

The utility fair optimization problem is to obtain optimum $[\theta_f]_{f\in\mathcal{F}}$, $[n_f]_{f\in\mathcal{F}}$, and $[k_f]_{f\in\mathcal{F}}$ for a given set of parameters $[[w_{f,c}]_{f\in\mathcal{F}_c}]_{c\in\mathcal{C}}$ and $[T_c]_{c\in\mathcal{C}}$, which is given by

$$\max_{\boldsymbol{\theta},(\mathbf{n},\mathbf{x})} \quad U(\boldsymbol{\theta},(\mathbf{n},\mathbf{x})) \tag{4}$$

$$\text{subject to} \quad \sum_{f:c\in\mathcal{C}_f} \frac{n_f}{w_{f,c}} \le T_c \qquad \forall c\in\mathcal{C} \tag{5}$$

$$\theta_f > 0 \qquad \forall f\in\mathcal{F} \tag{6}$$

$$x_f \le \overline{\lambda}_f \qquad \forall f\in\mathcal{F} \tag{7}$$

$$x_f \ge \underline{\lambda}_f \qquad \forall f\in\mathcal{F} \tag{8}$$

with $\boldsymbol{\theta} := [\theta_f]_{f\in\mathcal{F}}$ the vector of Chernoff parameters, $\mathbf{n} := [n_f]_{f\in\mathcal{F}}$ the vector of flow packet sizes, and $\mathbf{x} := [x_f]_{f\in\mathcal{F}}$ the vector of flow coding rates (where we recall that $x_f = (1-r_f)/2$). Equation (5) enforces the network capacity (or the flow schedulability) constraints, (6) the positivity constraint on the Chernoff parameters, and the constraints (7) and (8) are introduced for technical reasons that will be discussed in more detail shortly (see Section V-C).

For proportional fairness, we select the sum of the log of the flow throughputs as our network utility U. For flow f, the expected throughput is $D_f k_f(1-\widetilde{e}_f)$ symbols in every time interval of duration $D_f T_{d(f)}$ (we recall that $d(f)$ is the destination cell of flow f), which is the same as $k_f(1-\widetilde{e}_f)$ symbols every time interval of duration $T_{d(f)}$, where $D_f k_f$ is the information packet size and $\widetilde{e}_f$ the packet decoding error probability. As the exact expression of $\widetilde{e}_f$ is intractable, we use the upper bound for $\widetilde{e}_f$, which is e_f. Thus, the objective function is given by

$$\begin{aligned}U(\boldsymbol{\theta},(\mathbf{n},\mathbf{x})) &:= \sum_{f\in\mathcal{F}} \ln\left(k_f\left(1-e_f(\theta_f,n_f,x_f)\right)\right)\\ &= \sum_{f\in\mathcal{F}} \ln\left(n_f r_f\left(1-e_f(\theta_f,n_f,x_f)\right)\right)\\ &= \sum_{f\in\mathcal{F}} \ln\left(n_f(1-2x_f)\left(1-e_f(\theta_f,n_f,x_f)\right)\right)\\ &= \sum_{f\in\mathcal{F}} \ln(n_f) + \sum_{f\in\mathcal{F}} \ln(1-2x_f)\\ &\qquad + \sum_{f\in\mathcal{F}} \ln\left(1-e_f(\theta_f,n_f,x_f)\right).\end{aligned}$$

The optimization problem yields the proportional fair flow coding rates and coded packet size n_f. Since the PHY transmission rates $w_{f,c}$ are known parameters, the coded packet size is proportional to the airtime used by a flow (i.e., the airtime is given by $n_f/w_{f,c}$).

A. Nonconvexity

The objective function $U(\boldsymbol{\theta},(\mathbf{n},\mathbf{x}))$ is separable in $(\theta_f,(n_f,x_f))$ for each flow f. However, it can be readily verified that $\ln(1-e_f(\theta_f,n_f,x_f))$ is not jointly concave in $(\theta_f,(n_f,x_f))$, and so the optimization is nonconvex. Hence, the network utility maximization problem defined in (4)–(8) is not in the standard convex optimization framework.

B. Reformulation as Sequential Optimizations

We proceed by making the following key observation.

Lemma 3: For convex sets $\mathcal{Y}$ and $\mathcal{Z}$, and for a function $f:\mathcal{Y}\times\mathcal{Z}\to\mathbb{R}$ that is concave in $y\in\mathcal{Y}$ and in $z\in\mathcal{Z}$, but not jointly in (y,z), the solution to the joint optimization problem

$$\max_{y\in\mathcal{Y},z\in\mathcal{Z}} f(y,z) \tag{9}$$

is unique and is the same as the solution to

$$\max_{z\in\mathcal{Z}} \max_{y\in\mathcal{Y}} f(y,z) \tag{10}$$

if $f(y^*(z),z)$ is a concave function of z, where for each $z\in\mathcal{Z}$, $y^*(z) := \arg\max_{y\in\mathcal{Y}} f(y,z)$.

Proof: See Appendix C. □

This lemma establishes conditions under which we can transform a nonconvex optimization into a sequence of convex optimizations. Roughly speaking, we proceed by optimizing over each variable in turn and substituting the optimal variable value that is found back into the objective function. This creates a sequence of objective functions. Provided each member of this sequence is concave in the variable being optimized (but not necessary jointly concave in all variables), the solution to the sequence of convex optimizations coincides with the solution to the original nonconvex optimization. Evidently, the condition that concavity holds for every objective function in this sequence is extremely strong. Remarkably, however, we show that it is satisfied in our present network utility optimization.

C. Optimal $\boldsymbol{\theta}^*(x_f)$

Taking a sequential optimization approach, we begin by first solving the optimization

$$\begin{aligned} \max_{\boldsymbol{\theta}} \quad & U\left(\boldsymbol{\theta}, (\mathbf{n}, \mathbf{x})\right) \\ \text{subject to} \quad & \theta_f > 0 \qquad \forall f \in \mathcal{F} \end{aligned}$$

given packet sizes $n \in \mathbb{Z}_+^F$ and coding rates $\mathbf{x} \in [\underline{\lambda}_f, \overline{\lambda}_f]^F$. The objective function is separable and concave in the θ_f s. The partial derivative of $U\left(\boldsymbol{\theta}, (\mathbf{n}, \mathbf{x})\right)$ with respect to θ_f is given by

$$\frac{\partial U\left(\boldsymbol{\theta}, (\mathbf{n}, \mathbf{x})\right)}{\partial \theta_f} = \frac{e_f D_f n_f}{1 - e_f}\left[x_f - \frac{\beta_f e^{\theta_f}}{1 - \beta_f + \beta_f e^{\theta_f}}\right]. \quad (11)$$

Setting this derivative equal to zero, provided $x_f > \beta_f$ this is solved by

$$\begin{aligned} \frac{\beta_f e^{\theta_f^*}}{1 - \beta_f + \beta_f e^{\theta_f^*}} &= x_f \\ \text{or}, e^{\theta_f^*} &= \frac{x_f}{\beta_f}\frac{1 - \beta_f}{1 - x_f} \\ \text{or}, \theta_f^* &= \ln\left(\frac{x_f}{\beta_f}\right) - \ln\left(\frac{1 - x_f}{1 - \beta_f}\right). \quad (12) \end{aligned}$$

Observe that in fact θ_f^* is a function only of x_f and not both n_f and x_f. The requirement for $x_f > \beta_f$ ensures that $\theta_f^* > 0$. When $x_f \leq \beta_f$, the derivative (11) is negative for all $\theta_f > 0$. In this case, the optimum θ_f^* is zero, which yields an error probability e_f of one. Thus, for error recovery we require $x_f > \beta_f$, i.e., the coding rate $r_f < 1 - 2\beta_f$, and for a nonempty feasible region in the NUM problem formulation in (4)–(8), the constraints on x_f should satisfy the following: $\overline{\lambda}_f < 1 - 2\beta_f$ and $\underline{\lambda}_f > 0$. We note that the capacity region for a BSC having a crossover probability α_f with an m-ary signaling is $(0, m(1 - H(\alpha_f)))$, and the coding rate $1 - 2\beta_f$ lies in the capacity region.

D. Optimal (n_f^*, x_f^*)

The next step in our sequential optimization approach is to solve

$$\begin{aligned} \max_{(\mathbf{n},\mathbf{x})} \quad & U\left(\boldsymbol{\theta}^*(\mathbf{x}), (\mathbf{n}, \mathbf{x})\right) \\ \text{subject to} \quad & \sum_{f:c\in\mathcal{C}_f} \frac{n_f}{w_{f,c}} \leq T_c \qquad \forall c \in \mathcal{C} \\ & x_f \leq \overline{\lambda}_f \qquad \forall f \in \mathcal{F} \\ & x_f \geq \underline{\lambda}_f \qquad \forall f \in \mathcal{F}. \end{aligned}$$

That is, we substitute into the objective function for the optimal θ_f^* found in Section V-C. Defining $I_f = x_f \ln\left(\frac{x_f}{\beta_f}\right) + (1 - x_f)\ln\left(\frac{1-x_f}{1-\beta_f}\right)$

$$\begin{aligned} U\left(\boldsymbol{\theta}^*(\mathbf{x}), (\mathbf{n}, \mathbf{x})\right) = &\sum_{f\in\mathcal{F}} \ln(n_f) + \sum_{f\in\mathcal{F}} \ln(1 - 2x_f) \\ &+ \sum_{f\in\mathcal{F}} \ln\left(1 - e^{-D_f n_f I_f}\right). \end{aligned}$$

It can be verified that $U\left(\boldsymbol{\theta}^*(\mathbf{x}), (\mathbf{n}, x)\right)$ is not jointly concave in $(\mathbf{n}, \mathbf{x})$. To proceed, we therefore rewrite the objective in terms of the log-transformed variables $\widetilde{n}_f = \ln(n_f)$ and $\widetilde{I}_f = \ln(I_f)$. Observe that the mapping from n_f to $\widetilde{n}_f$ is invertible, and similarly the mapping from x_f to $\widetilde{I}_f$. Since $\widetilde{I}_f$ is a monotone increasing function of x_f (this can be verified by inspection of the first derivative), the inverse mapping from $\widetilde{I}_f$ to x_f exists and is one-to-one. With the obvious abuse of notation, we write inverse map as $x_f(\widetilde{I}_f)$. In terms of these log-transformed coordinates, the objective function is $U\left(\boldsymbol{\theta}^*(\tilde{\mathbf{I}}), (\tilde{\mathbf{n}}, \tilde{\mathbf{I}})\right)$. We note that the problem defined in (4)–(8) is equivalent to the problem

$$\begin{aligned} \max_{\boldsymbol{\theta},(\tilde{\mathbf{n}},\tilde{\mathbf{I}})} \quad & U\left(\boldsymbol{\theta}, (\tilde{\mathbf{n}}, \tilde{\mathbf{I}})\right) \\ \text{subject to} \quad & \sum_{f:c\in\mathcal{C}_f} \frac{e^{\tilde{n}_f}}{w_{f,c}} \leq T_c \quad \forall c \in \mathcal{C} && (13) \\ & \theta_f > 0 \qquad \forall f \in \mathcal{F} && (14) \\ & \tilde{I}_f \leq \overline{\tilde{\lambda}}_f \qquad \forall f \in \mathcal{F} && (15) \\ & \tilde{I}_f \geq \underline{\tilde{\lambda}}_f \qquad \forall f \in \mathcal{F} && (16) \end{aligned}$$

and hence, by Lemma 3, the solution to the log-transformed problem is the same as that of the problem defined in (4)–(8). We solve the maximization problem by convex optimization method. We show that the objective function is jointly concave in $\left(\tilde{n}, \tilde{I}\right)$ in the following lemma.

Lemma 4:

$$\begin{aligned} U\left(\boldsymbol{\theta}^*(\tilde{\mathbf{I}}), (\tilde{\mathbf{n}}, \tilde{\mathbf{I}})\right) = &\sum_{f\in\mathcal{F}} \tilde{n}_f + \sum_{f\in\mathcal{F}} \ln\left(1 - 2x_f(\widetilde{I}_f)\right) \\ &+ \sum_{f\in\mathcal{F}} \ln\left(1 - e^{-D_f e^{\tilde{n}_f + \tilde{I}_f}}\right) \end{aligned}$$

is jointly concave in $\widetilde{n}_f$ and $\widetilde{I}_f$.

Proof: See Appendix D. □

Hence, we have the following convex optimization problem:

$$\begin{aligned} \max_{(\tilde{\mathbf{n}},\tilde{\mathbf{I}})} \quad & U\left(\boldsymbol{\theta}^*(\tilde{\mathbf{I}}), (\tilde{\mathbf{n}}, \tilde{\mathbf{I}})\right) && (17) \\ \text{subject to} \quad & \sum_{f:c\in\mathcal{C}_f} \frac{e^{\widetilde{n}_f}}{w_{f,c}} \leq T_c \qquad \forall c \in \mathcal{C} && (18) \\ & \tilde{I}_f \leq \overline{\tilde{\lambda}}_f \qquad \forall f \in \mathcal{F} && (19) \\ & \tilde{I}_f \geq \underline{\tilde{\lambda}}_f \qquad \forall f \in \mathcal{F}. && (20) \end{aligned}$$

We solve the above maximization problem using the Lagrangian relaxation approach. The Lagrangian function of the problem is

given by

$$L\left(\widetilde{\mathbf{n}},\widetilde{\mathbf{I}},\mathbf{p},\underline{\boldsymbol{\nu}},\overline{\boldsymbol{\nu}}\right)$$
$$:=\sum_{f\in\mathcal{F}}U_f(\theta_f^*(\widetilde{I}_f),(\widetilde{n}_f,\widetilde{I}_f))-\sum_{c\in\mathcal{C}}p_c\left(\sum_{f\in\mathcal{F}_c}\frac{e^{\widetilde{n}_f}}{w_{f,c}}-T_c\right)$$
$$-\sum_{f\in\mathcal{F}}\underline{\nu}_f\left(\tilde{I}_f-\overline{\tilde{\lambda}}_f\right)+\sum_{f\in\mathcal{F}}\overline{\nu}_f\left(\tilde{I}_f-\underline{\tilde{\lambda}}_f\right)$$

where $\mathbf{p}\geq\mathbf{0},\underline{\boldsymbol{\nu}}\geq\mathbf{0}$, and $\overline{\boldsymbol{\nu}}\geq\mathbf{0}$ are Lagrangian multipliers corresponding to the constraints given in (18)–(20). The channel error probabilities β_f's are strictly positive, and the channel coding rates are always assumed to be in the interior of the feasibility region. Hence, the constraints for the channel coding rate given in (19) and (20) are not active at the optimal point, and the Lagrangian costs $\underline{\nu}_f$'s and $\overline{\nu}_f$'s are zero. Thus, the shadow costs corresponding to these constraints will not appear in the Lagrangian relaxation.

Since the optimization problem falls within convex optimization framework, and the Slater condition is satisfied, strong duality holds. Hence, the KKT conditions are necessary and sufficient for optimality. Differentiating the Lagrangian with respect to $\widetilde{n}_f$ at $\widetilde{n}_f=\widetilde{n}_f^*$, and setting equal to zero yields the KKT condition

$$1+\frac{D_f\exp(\widetilde{n}_f^*+\widetilde{I}_f^*)e^{-D_f\exp(\widetilde{n}_f^*+\widetilde{I}_f^*)}}{1-e^{-D_f\exp(\widetilde{n}_f^*+\widetilde{I}_f^*)}}=\sum_{c\in\mathcal{C}_f}\frac{p_ce^{\widetilde{n}_f^*}}{w_{f,c}}$$
$$\text{or,}\quad 1+\frac{D_fn_f^*I_f(x_f^*)e^{-D_fn_f^*I_f(x_f^*)}}{1-e^{-D_fn_f^*I_f(x_f^*)}}=\sum_{c\in\mathcal{C}_f}\frac{p_cn_f^*}{w_{f,c}}. \quad (21)$$

Similarly, the KKT condition for $\widetilde{I}_f^*$ is

$$\frac{D_f\exp(\widetilde{n}_f^*+\widetilde{I}_f^*)e^{-D_f\exp(\widetilde{n}_f^*+\widetilde{I}_f^*)}}{1-e^{-D_f\exp(\widetilde{n}_f^*+\widetilde{I}_f^*)}}=\frac{2}{1-2x_f^*}\frac{I_f^*}{\theta_f^*}$$

or

$$\frac{D_fn_f^*I_f(x_f^*)e^{-D_fn_f^*I_f(x_f^*)}}{1-e^{-D_fn_f^*I_f(x_f^*)}}=\frac{2}{1-2x_f^*}\frac{I_f(x_f^*)}{\theta_f^*(x_f^*)}. \quad (22)$$

Combining (21) and (22) yields

$$\sum_{c\in\mathcal{C}_f}\frac{p_cn_f^*}{w_{f,c}}-1=\frac{2}{1-2x_f^*}\frac{I_f(x_f^*)}{\theta_f^*(x_f^*)}. \quad (23)$$

Observe that the left-hand side (LHS) is a function of n_f^* and the right-hand side (RHS) is a function of x_f^*. Thus, the choice of packet size parameter n_f^* and coding rate parameter x_f^* are, in general, coupled.

E. Distributed Algorithm for Solving Optimization

Given the values of the Lagrange multipliers $\mathbf{p}^*$, the solution to (23) specifies the optimal packet size and coding rate. To complete the solution to the optimization, it therefore remains to calculate the multipliers $\mathbf{p}^*$. These cannot be obtained in closed form since their values reflect the network topology and details of flow routing. However, they can be readily found in a distributed manner using a standard subgradient approach.

We proceed as follows. The dual problem for the primal problem defined in (17) is given by

$$\min_{\mathbf{p}\geq0}\quad D(\mathbf{p})$$

where the dual function $D(\mathbf{p})$ is given by

$$\begin{aligned}D(\mathbf{p})&=\max_{(\widetilde{\mathbf{n}},\widetilde{\mathbf{I}})}\sum_{f\in\mathcal{F}}U_f(\theta_f^*(\widetilde{I}_f),(\widetilde{n}_f,\widetilde{I}_f))\\&\qquad+\sum_{c\in\mathcal{C}}p_c\left(T_c-\sum_{f\in\mathcal{F}_c}\frac{e^{\widetilde{n}_f}}{w_{f,c}}\right)\\&=\sum_{f\in\mathcal{F}}U_f\left(\theta_f^*(\widetilde{I}_f(p)),(\widetilde{n}_f^*(\mathbf{p}),\widetilde{I}_f^*(\mathbf{p}))\right)\\&\qquad+\sum_{c\in\mathcal{C}}p_c\left(T_c-\sum_{f\in\mathcal{F}_c}\frac{e^{\widetilde{n}_f^*(\mathbf{p})}}{w_{f,c}}\right).\end{aligned} \quad (24)$$

From (24), for any $(\widetilde{\mathbf{n}},\widetilde{\mathbf{I}})$

$$D(\mathbf{p})\geq\sum_{f\in\mathcal{F}}U_f(\theta_f^*(\widetilde{I}_f),(\widetilde{n}_f,\widetilde{I}_f))+\sum_{c\in\mathcal{C}}p_c\left(T_c-\sum_{f\in\mathcal{F}_c}\frac{e^{\widetilde{n}_f}}{w_{f,c}}\right)$$

and in particular, the dual function $D(\mathbf{p})$ is greater than that for $\widetilde{I}_f=\widetilde{I}_f^*(\widetilde{\mathbf{p}})$ for some arbitrary $\widetilde{\mathbf{p}}$, i.e.,

$$\begin{aligned}D(\mathbf{p})&\geq\sum_{f\in\mathcal{F}}U_f\left(\theta_f^*(\widetilde{I}_f^*(\widetilde{\mathbf{p}})),(\widetilde{n}_f^*(\widetilde{\mathbf{p}}),\widetilde{I}_f^*(\widetilde{\mathbf{p}}))\right)\\&\qquad+\sum_{c\in\mathcal{C}}p_c\left(T_c-\sum_{f\in\mathcal{F}_c}\frac{e^{\widetilde{n}_f^*(\widetilde{\mathbf{p}})}}{w_{f,c}}\right)\\&=D(\widetilde{\mathbf{p}})+\sum_{c\in\mathcal{C}}(p_c-\widetilde{p}_c)\left(T_c-\sum_{f\in\mathcal{F}_c}\frac{e^{\widetilde{n}_f^*(\widetilde{\mathbf{p}})}}{w_{f,c}}\right).\end{aligned} \quad (25)$$

Thus, a subgradient of $D(\cdot)$ at any $\widetilde{\mathbf{p}}$ is given by the vector

$$\left[T_c-\sum_{f\in\mathcal{F}_c}\frac{n_f^*(\widetilde{\mathbf{p}})}{w_{f,c}}\right]_{c\in\mathcal{C}}$$

and the projected subgradient descent update is

$$p_c(i+1)=\left[p_c(i)-\gamma\cdot\left(T_c-\sum_{f\in\mathcal{F}_c}\frac{n_f^*(\mathbf{p}(i))}{w_{f,c}}\right)\right]^+$$

where $\gamma>0$ is a sufficiently small stepsize, and $[f(x)]^+:=\max\{f(x),0\}$ ensures that the Lagrange multiplier never goes negative (see [11]).

The subgradient updates can carried out locally by each cell c since the update of p_c only requires knowledge of the packet sizes $n_f^*(\mathbf{p}(i))$ of flows $f\in\mathcal{F}_c$ traversing cell c. Thus, at the beginning of each iteration i, the flow source nodes choose their packet sizes as $D_fn_f^*(\mathbf{p}(i))$ and the coding rates as $1-2x_f^*(\mathbf{p}(i))$, and each cell computes its cost based on the packet sizes (or equivalently the rates) of flows through it. The updated costs along the route of each flow are then fed back to the source

nodes to compute the packet size and coding rate for the next iteration.

Observe that the Lagrange multiplier p_c can be interpreted as the cost of transmitting traffic through cell c. The amount of service time that is available is given by $\Delta = T_c - \sum_{f\in\mathcal{F}_c} \frac{n_f^*(\mathbf{p}(i))}{w_{f,c}}$. When Δ is positive and large, then the Lagrangian cost p_c decreases rapidly (because the dual function $D(\cdot)$ is convex), and when Δ is negative, then the Lagrangian cost p_c increases rapidly to make $\Delta \geq 0$. We note that the increase or decrease of p_c between successive iterations is proportional to Δ, the amount of service time available. Thus, the subgradient procedure provides a dynamic control scheme to balance the network load.

The resulting distributed implementation of the joint airtime/coding rate optimization is summarized in Algorithm 1.

Algorithm 1 Distributed Implementation of Joint Airtime/Coding Rate Optimization.

Each cell c runs:
loop
1.

$$p_c(i+1) = \left[p_c(i) - \gamma \cdot \left(T_c - \sum_{f\in\mathcal{F}_c} \frac{n_f^*(\mathbf{p}(i))}{w_{f,c}} \right) \right]^+$$

end loop
The source for each flow f runs:
loop
1. Measure $\sum_{c\in\mathcal{C}_f} \frac{p_c}{w_{f,c}}$, the aggregate cost of using the cells along the route of flow f. E.g., if each cell updates the header of transmitted packets to reflect this sum, it can then be echoed back to the source by the flow destination.
2. Find the unique packet size n_f^* and coding rate x_f^* that solve (23). Since there are only two variables, a simple numerical search can be used.

end loop

VI. Two Special Cases

A. Delay-Insensitive Networks

Suppose the delay deadline $D_f \to \infty$ for all flows. For any positive bounded $n_f^* I_f^*$, i.e., $0 < n_f^* I_f^* < \infty$, the LHS of (22) can be written as

$$\begin{aligned}\frac{D_f n_f^* I_f^* e^{-D_f n_f^* I_f^*}}{1 - e^{-D_f n_f^* I_f^*}} &= \frac{D_f n_f^* I_f^*}{e^{D_f n_f^* I_f^*} - 1} \\ &= \frac{D_f n_f^* I_f^*}{\sum_{j=1}^{\infty} \frac{(D_f n_f^* I_f^*)^j}{j!}} \\ &= \frac{1}{1 + \sum_{j=2}^{\infty} \frac{(D_f n_f^* I_f^*)^{j-1}}{j!}}\end{aligned}$$

$$\therefore \lim_{D_f\to\infty} \frac{D_f n_f^* I_f^* e^{-D_f n_f^* I_f^*}}{1 - e^{-D_f n_f^* I_f^*}} = 0. \tag{26}$$

Thus, the asymptotic optimal coding rate x_f^* as the delay deadline requirement $D_f \to \infty$ is the solution to

$$\frac{2}{1-2x_f^*} \frac{I_f(x_f^*)}{\theta^*(x_f^*)} = 0. \tag{27}$$

Since $\beta_f < x_f < 1/2$, it is sufficient to find the solution to

$$\frac{I_f(x_f^*)}{\theta^*(x_f^*)} = 0.$$

$$\text{Note that} \quad \lim_{x_f^*\to\beta_f} \frac{I_f(x_f^*)}{\theta^*(x_f^*)} = 0$$

$$\text{and hence} \quad \lim_{D_f\to\infty} x_f^* = \beta_f. \tag{28}$$

Since this is the limiting solution and $x_f^* > \beta_f$, one can use $x_f^* = \beta_f + \epsilon$ for some arbitrarily small $\epsilon > 0$. Similarly, from (21), the asymptotic optimal packet size n_f^* as $D_f \to \infty$ is

$$n_f^* = \frac{1}{\sum_{c\in C_f} p_c / w_{f,c}} \tag{29}$$

where the multipliers p_c are obtained, as before, by subgradient descent

$$p_c(i+1) = \left[p_c(i) - \gamma \cdot \left(T_c - \sum_{f\in\mathcal{F}_c} \frac{n_f^*(\mathbf{p}(i))}{w_{f,c}} \right) \right]^+. \tag{30}$$

Observe that the optimal coding rate $x_f^* = \beta_f + \epsilon$ that is given by the solution of (28) is determined solely by the channel error rate β_f of flow f. It is therefore completely independent of the other network properties. In particular, it is independent of the packet size n_f^* used, of the other flows sharing the network, and of the network topology. Conversely, observe that the optimal packet size n_f^* in (29) and (30) is dependent on the network topology and flow routes, but is completely independent of the error rate β_f and coding rate x_f. That is, in delay-insensitive networks, the joint airtime/coding rate optimization task breaks into separate optimal airtime allocation and optimal coding rate allocation tasks that are completely decoupled. Our optimization therefore yields a MAC/PHY layering, whereby airtime allocation/transmission scheduling is handled by the MAC, whereas coding rate selection is handled by the PHY, with no cross-layer communication. It is important to note, however, that this layering does not occur in networks where one or more flows have finite delay deadlines; see Section VII for a more detailed discussion.

B. Loss-Free Networks

Suppose the channel symbol error rate $\beta_f = 0$ for all flows. From (12), we observe that

$$\lim_{\beta_f\to 0} \theta_f^* = \infty \tag{31}$$

and this yields $e_f = 0$ for all flows. The objective function in (17) degenerates to $\sum_{f\in\mathcal{F}} \ln(n_f(1-2x_f))$. We note that for any $x_f^* > \beta_f > 0$, as $\beta_f \downarrow 0$, $I_f(x_f^*) \to \infty$. Hence, the LHS of (22) becomes

$$\lim_{\beta_f\downarrow 0} \frac{D_f n_f^* I_f(x_f^*) e^{-D_f n_f^* I_f(x_f^*)}}{1 - e^{-D_f n_f^* I_f(x_f^*)}} = 0. \tag{32}$$

In the same way as in (28), this limit can be achieved by $x_f^* = 0$ (i.e., $r_f^* = 1$). Similarly, the optimal packet size is $n_f^* = \frac{1}{\sum_{c \in \mathcal{C}_f} p_c / w_{f,c}}$. This optimal packet size is identical to that for delay-insensitive networks—see (29)—and it can be verified that in fact it corresponds to the classical proportional fair rate allocation for loss-free networks, as expected.

VII. Examples

A. Single Cell

We begin by considering network examples consisting of a single cell carrying multiple flows. The network topology is illustrated schematically in Fig. 1 and might correspond, for example, to a WLAN.

1) Mix of Delay-Sensitive and Delay-Insensitive Flows: Suppose the flows in the network belong to two classes, one of which is delay-sensitive and has a delay-deadline D, whereas the other is delay-insensitive, i.e., has an infinite delay deadline. These classes might correspond, for example, to video and data traffic. Fig. 3(a) plots the optimal airtime allocation as the delay deadline D is varied. In this example, there is a single delay-sensitive flow and two delay-insensitive flows, and the airtime allocation is shown for the delay-sensitive flow and for one of the delay-insensitive flows (both receive the same airtime allocation). As expected, it can be seen that the airtime allocations of the delay-sensitive and delay-insensitive flows approach each other as the delay deadline D is increased. However, it is notable that they approach each other fairly slowly, and when the delay deadline is low, the airtime allocated to the delay-sensitive flow is almost 50% greater than that allocated to a delay-insensitive flow. This behavior is qualitatively different from the classical proportional fair allocation neglecting coding rate and delay deadlines, which would allocate equal airtime to all flows. By taking coding rate and delay deadlines into account, our approach allows the resource allocation to flows with different quality-of-service requirements to be carried out in a principled and fair manner.

Fig. 3(b) plots the optimal airtime allocation as the number N of delay-insensitive flows is varied. It can be seen that the airtime allocated to each flow decreases as N is increased, as expected since the number of flows sharing the network is increasing. Interestingly, observe that the airtime allocated to the delay-sensitive flow is a roughly constant margin above that allocated to the delay-insensitive flows. The delay-sensitive flow is therefore "protected" from the delay-insensitive flows. However, in contrast to *ad hoc* approaches, this protection is carried out in a principled and fair manner.

2) Mix of Near and Far Stations: Consider now a situation where all flows have the same delay deadline D, but where for some flows the sources are located close to the destination, and for other flows, the sources are further away. We therefore have two classes of flows, one with a higher channel symbol error rate than the other when both use the same PHY rate. Fig. 4(a) plots the optimal airtime allocation for a flow in each class as the channel error rate for one class is varied. When the channel error rates for both classes are the same ($\beta_f = 10^{-2}$), it can be seen that the airtime allocation is the same. As the channel error rate decreases, the airtime allocated to flow 1 decreases. Conversely, as the channel error rate increases, the airtime allocated to flow 1 increases.

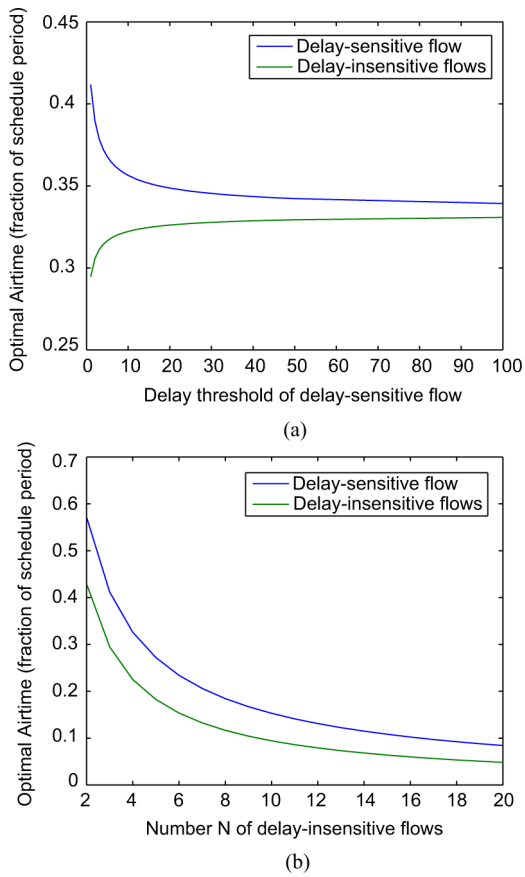

Fig. 3. Single WLAN with one delay-sensitive flow and N delay-insensitive flows. Delay-sensitive flow has delay deadline D; delay-insensitive flows have infinite delay deadlines. Raw channel symbol error rate is 10^{-2} for all flows; PHY rate for all flows is 10 symbols per schedule period. Optimal airtimes are given as a proportion of the schedule period. (a) Optimal airtime allocation versus delay deadline D, $N = 2$. (b) Optimal airtime allocation versus N. $D = 1$.

Fig. 4(b) plots the optimal airtime allocation when flows in both classes have the same channel error rate but different PHY rates, i.e., where the PHY modulation has been adjusted to equalize the channel error rates. When the PHY rates are the same ($w_{f,c} = 10$ symbols per schedule period), the airtime allocation is the same to both classes. As the PHY rate is increased, the airtime allocation for flow 1 decreases. Conversely, as the PHY rate is decreased, the airtime allocation for flow 1 increases. Again, note that this is qualitatively different from the classical proportional fair allocation neglecting coding rate and delay deadlines that would allocate equal airtime to all flows.

3) Unequal Airtime: The basic observations in these examples apply more generally. In particular, as noted above, in a loss-free, delay-insensitive single cell network, the proportional fair allocation is to assign equal airtime to all flows ([3] and Section VI-B). However, when delay deadlines are introduced and/or links are lossy, we see an interesting phenomenon.

Lemma 5: The optimum rate allocation $\mathbf{x}^*$ (or equivalently $\mathbf{r}^*$) is not equivalent to an equal airtime allocation.

Proof: See Appendix E. □

In particular, flows that see a better channel get less airtime than flows that see a worse channel.

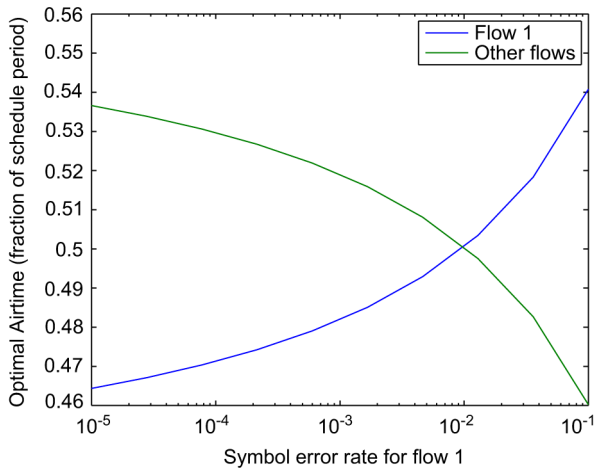

(a)

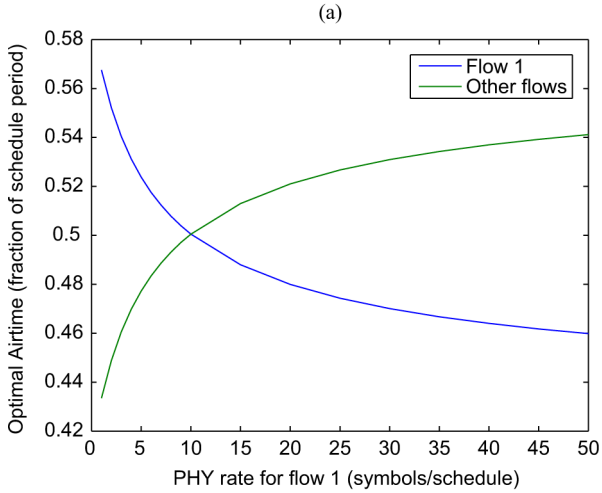

(b)

Fig. 4. Single WLAN with two delay-sensitive flows, both with delay deadline $D = 1$. In (a), PHY rate for both flows is 10 symbols per schedule period, and channel symbol error rate for flow 1 is varied. In (b), channel symbol error rate for both flows is 10^{-2}, and PHY rate for flow 1 is varied. (a) Optimal airtime allocation versus channel symbol error rate for flow 1; symbol error rate for flow 2 is held fixed at 10^{-2}. (b) Optimal airtime allocation versus PHY rate of flow 1; PHY rate for flow 2 is held fixed at 10 symbols/schedule.

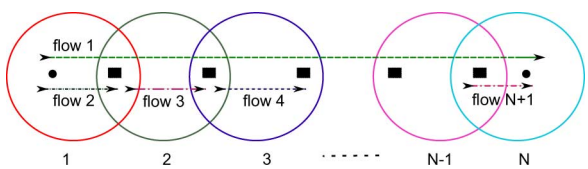

Fig. 5. Linear Parking Lot network with N cells and $N+1$ flows (one multihop flow and N single-hop flows).

B. Multiple Cells

We now consider a mesh network consisting of N cells carrying $N + 1$ flows in the well-studied Parking Lot topology. The network topology is illustrated in Fig. 5. The flows in this network can be assigned to two classes: Class 1 consists of the N-hop flow, and class 2 consists of the single-hop flows 2, 3, $\cdots$, $N + 1$. Each cell has the same schedule period, i.e., $T_c = T, \forall c \in \mathcal{C}$.

1) Impact of Number of Hops: Suppose that both classes of flows use the same symbol transmission PHY rate and experience the same loss rate in each cell. Then, the N-hop flow will experience a higher end-to-end symbol error rate than the single-hop flows, and the loss rate will increase with N. Fig. 6 plots the ratio of optimal airtime allocated to each class of flow versus N. Results are shown for three delay-deadline requirements: Both classes of flow are delay-sensitive with delay deadline $D_1 = D_2 = 1$; class 1 is delay-sensitive ($D_1 = 1$), while class 2 is delay-insensitive ($D_2 = 10^5$); class 1 is delay-insensitive, while class 2 is delay-sensitive. It can be seen that in the first case, where both classes have the same delay deadline, the ratio of airtime is larger than 1. This is in accordance with the previous observation that flows with poorer channel conditions are allocated more airtime than flows with better channel conditions. In the second case, where class 2 is delay-insensitive ($D_2 = 10^5$), additional airtime is allocated to class 1, the delay-sensitive flow, which also corresponds with the single-cell analysis. In the third case, where class 1 is delay-insensitive ($D_1 = 10^5$) and class 2 is delay-sensitive, it can be seen that class-2 flows are allocated slightly more airtime that the class-1 flow. Interestingly, however, observe that the airtime allocated to the class-1 flow is insensitive to the number N of hops. This contrasts with the behavior when the class-1 flow is delay-sensitive.

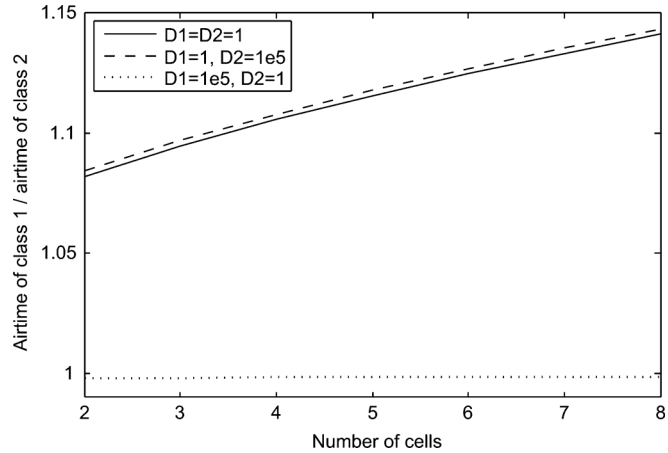

Fig. 6. Ratio of airtime versus number N of cells in Parking Lot topology of Fig. 5. The y-axis is the ratio of the airtime allocated to the N-hop flow to that allocated to a single hop flow; note that the airtime of the N-hop flow is the sum of allocated airtime in each cell along the flows route. Data are shown for three different delay deadline requirements, as indicated in the legend. All flows have the same PHY rate.

2) Impact of Different Flow PHY Rates: Now consider a situation where the number of cells $N = 3$ and all flows have the same delay deadline $D_1 = D_2 = 1$. Flows 2 and 4 have symbol error rate 10^{-4}, and flows 1 and 3 have symbol error rate 2.5×10^{-1}. We classify the flows into three sets: Class 1 consists of multihop flow 1, class 2 consists of single-hop flows 2 and 4, and class 3 consists of single-hop flow 3. Let w denote the PHY rate used used by class-1 and class-2 flows, and w_3 denote the PHY rate used by the class-3 flow. Fig. 7 plots the optimal coded packet size versus the ratio w_3/w. We begin by observing that when $w_3/w = 1$, all flows have the same PHY rate, and it can be seen that flows in classes 2 and 3 are allocated the same packet sizes (and so the same airtime). Hence, although the flow in class 3 crosses a much more lossy link than the flows in class 2, the optimal allocation ensures that all of the single-hop flows have the same airtime. The multihop flow in class 1 is allocated a smaller packet size (and so less airtime)

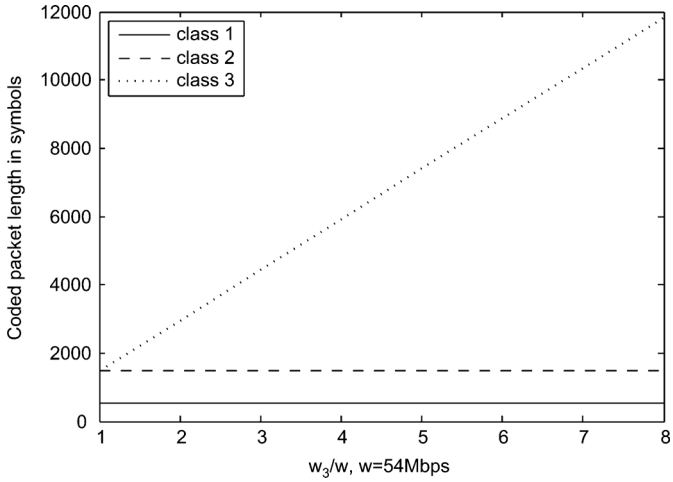

Fig. 7. Coded packet size versus ratio of PHY rates w_3/w for Parking Lot topology of Fig. 5 with $N = 3$ cells. Class 1 consists of multihop flow 1, class 2 consists of single-hop flows 2 and 4, and class 3 consists of single-hop flow 3. Class-1 and 2 flows use PHY rate w bit/s; the class-3 flow uses a PHY rate of w_3 bit/s. All flows have delay deadline $D = 1$.

than the single-hop flows. It can also be seen that varying the PHY rate for the single-hop flow in class 3 does not affect the optimal coded packet sizes of flows in classes 1 and 2, and hence the airtime of class-1 and class-2 flows remains the same as w_3 is varied. The coded packet size of the class-3 flow increases linearly with w_3/w, and so the airtime of the class-4 flow remains invariant as well.

VIII. Conclusion

In this paper, we posed a utility fair problem that yields the optimum airtime and the coding rate across flows in a capacity constrained multihop network with delay deadlines. We showed that the problem is highly nonconvex. Nevertheless, we demonstrate that the global network utility optimization problem can be solved. We obtained the optimum airtime/packet size and channel coding rate and analyzed its properties. A key result is that in the presence of channel errors, even in a single cell case, the proportional fair allocations of airtime across flows are different (which, in the loss-free channel, is the same). We also analyzed some simple networks based on the utility optimum framework we proposed. To the best of our knowledge, this is the first work on cross-layer optimization that studies optimum coding across flows that are competing for network resources and have delay-deadline constraints.

Appendix A
Proof of Lemma 1

From the definition of $\widetilde{e}_f$

$$\begin{aligned}
\widetilde{e}_f &= \mathbb{P}\left\{\sum_{i=1}^{D_f n_f} E_f[i] > \frac{D_f n_f - D_f k_f}{2}\right\} \\
&= \mathbb{P}\left\{\sum_{i=1}^{D_f n_f} E_f[i] > D_f n_f \left(\frac{1-r_f}{2}\right)\right\} \\
&\overset{a}{\leqslant} \exp\left(-D_f n_f \cdot \theta_f \frac{1-r_f}{2}\right) \mathbb{E}\left[\exp\left(\theta_f \sum_{i=1}^{D_f n_f} E_f[i]\right)\right] \\
&\overset{b}{=} \exp\left(-D_f n_f \cdot \theta_f \frac{1-r_f}{2}\right) \left[\mathbb{E}\left[\exp\left(\theta_f E_f[1]\right)\right]\right]^{D_f n_f} \\
&= \exp\left(-D_f n_f \cdot \theta_f \frac{1-r_f}{2}\right) \exp\left(D_f n_f \ln\left(\mathbb{E}\left[e^{\theta_f E_f[1]}\right]\right)\right) \\
&= \exp\left(-D_f n_f \left[\theta_f \frac{1-r_f}{2} - \ln\left(\mathbb{E}\left[e^{\theta_f E_f[1]}\right]\right)\right]\right) \\
&= \exp\left(-D_f n_f I_{E_f[1]}\left(\frac{1-r_f}{2}; \theta_f\right)\right).
\end{aligned}$$

In the derivation above, in step a, we applied Markov's inequality, and in step b, we applied the independence of the random variables $E_f[1], E_f[2], \ldots, E_f[D_f n_f]$. ■

Appendix B
Proof of Lemma 2

From the definition of $\widetilde{e}_f$

$$\begin{aligned}
\widetilde{e}_f &= \mathbb{P}\left\{\sum_{i=1}^{D_f n_f} E_f[i] > \frac{D_f n_f - D_f k_f}{2}\right\} \\
&= \mathbb{P}\left\{\sum_{i=1}^{D_f n_f} E_f[i] > D_f n_f \frac{1-r_f}{2}\right\} \\
&= \sum_{i=D_f n_f \frac{1-r_f}{2}+1}^{D_f n_f} \binom{D_f n_f}{i} \beta_f^i (1-\beta_f)^{D_f n_f - i}.
\end{aligned}$$

The binomial coefficients can be bounded as follows:

$$1 \leqslant \binom{n}{k} = \frac{n(n-1)\cdots(n-k+1)}{1 \cdot 2 \cdots k} \leqslant n^k.$$

Hence

$$\begin{aligned}
\widetilde{e}_f &\geqslant \sum_{i=D_f n_f \frac{1-r_f}{2}+1}^{D_f n_f} \beta_f^i (1-\beta_f)^{D_f n_f - i} \\
&\geqslant \frac{\beta_f}{1-\beta_f} \beta_f^{D_f n_f (\frac{1-r_f}{2})} (1-\beta_f)^{D_f n_f (\frac{1+r_f}{2})} \\
&= \frac{\beta_f}{1-\beta_f} \exp\left(-D_f n_f \left[\left(\frac{1-r_f}{2}\right) \ln(1/\beta_f)\right]\right) \\
&\quad \exp\left(-D_f n_f \left[\left(\frac{1+r_f}{2}\right) \ln(1/(1-\beta_f))\right]\right) \\
&= \frac{\beta_f}{1-\beta_f} \exp\left(-D_f n_f \left[\left(\frac{1-r_f}{2}\right) \ln\left(\frac{1-r_f}{2\beta_f}\right)\right]\right) \\
&\quad \exp\left(-D_f n_f \left[\left(\frac{1+r_f}{2}\right) \ln\left(\frac{1+r_f}{2(1-\beta_f)}\right)\right]\right) \\
&\quad \cdot \exp\left(D_f n_f \left[\left(\frac{1-r_f}{2}\right) \ln\left(\frac{1-r_f}{2}\right)\right]\right) \\
&\quad \cdot \exp\left(D_f n_f \left[\left(\frac{1+r_f}{2}\right) \ln\left(\frac{1+r_f}{2}\right)\right]\right) \\
&= \frac{\beta_f}{1-\beta_f} \exp\left(-D_f n_f H\left(\mathcal{B}\left(\frac{1-r_f}{2}\right)\right)\right) \\
&\quad \exp\left(-D_f n_f I\left(\mathcal{B}\left(\frac{1-r_f}{2}\right) \| \mathcal{B}(\beta_f)\right)\right).
\end{aligned}$$

Note that $\mathcal{B}(x)$ is the Bernoulli distribution with parameter x, $H(\mathcal{P})$ is the entropy of probability mass function (pmf) $\mathcal{P}$, and $I(\mathcal{P}\|\mathcal{Q})$ is the information divergence between the pmfs $\mathcal{P}$ and $\mathcal{Q}$. ■

Appendix C
Proof of Lemma 3

For any $z \in \mathcal{Z}$, the function $f(y,z)$ is concave in y. Hence, for each z, there exists a unique maximum $y^+(z)$, which is given by

$$\begin{aligned} f(y^+(z),z) &= \max_{y\in\mathcal{Y}} f(y,z) \\ &=: g(z). \end{aligned}$$

If $f(y^+(z),z)$ is a concave function of z, then there exists a unique maximizer, which is denoted by z^+, i.e.,

$$z^+ = \arg\max_{z\in\mathcal{Z}} f(y^+(z),z).$$

We show that $(y^+(z^+),z^+)$ is an optimum solution to (9). Since z^+ is the maximizer of g, we have for any $z \in \mathcal{Z}$

$$g(z^+) \geqslant g(z)$$

or

$$f(y^+(z^+),z^+) \geqslant f(y^+(z),z).$$

For any given $z \in \mathcal{Z}$, $y^+(z)$ is the maximizer of $f(y,z)$ over all $y \in \mathcal{Y}$, i.e.,

$$f(y^+(z),z) \geqslant f(y,z)$$

and hence, for all $(y,z) \in \mathcal{Y}\times\mathcal{Z}$

$$f(y^+(z^+),z^+) \;\geqslant\; f(y^+(z),z) \;\geqslant\; f(y,z).$$

We note that $y^+(\cdot)$ maps $\mathcal{Z}$ into $\mathcal{Y}$, and hence, $(y^+(z^+),z^+) \in \mathcal{Y}\times\mathcal{Z}$. Hence, $(y^+(z^+),z^+)$ is a global maximizer. ■

Appendix D
Proof of Lemma 4

Consider the optimization problem

$$\max_{\widetilde{\mathbf{n}},\widetilde{\mathbf{I}}} \sum_{f\in\mathcal{F}} \widetilde{n}_f + \ln(1-2x_f(\widetilde{I}_f)) + \ln(1-e^{-D_f\exp(\widetilde{n}_f+\widetilde{I}_f)})$$

$$\text{s.t.} \sum_{f:c\in\mathcal{C}_f} \frac{e^{\widetilde{n}_f}}{w_{f,c}} \leqslant T_c \qquad \forall c\in\mathcal{C}.$$

We show that the objective function is jointly (strictly) concave in $(\widetilde{\mathbf{n}},\widetilde{\mathbf{I}})$. The objective function is separable in $(\widetilde{n}_f,\widetilde{I}_f)$, and we show that $x_f(\widetilde{I}_f)$ is convex, and $\ln(1-e^{-D_f\exp(\widetilde{n}_f+\widetilde{I}_f)})$ is concave.

Since, for $x_f \in (\beta_f, 0.5)$, I_f is a monotone function of x_f, and $\widetilde{I}_f$ is a monotone function of I_f, it is clear that $\widetilde{I}_f$ is invertible. Note that

$$\begin{aligned} \widetilde{I}_f &= \ln(I_f) \\ \frac{d\widetilde{I}_f}{dx_f} &= \frac{\theta_f^*(x_f)}{I_f} \\ \frac{dx_f}{d\widetilde{I}_f} &= \frac{I_f}{\theta_f^*(x_f)} \\ \frac{d^2x_f}{d\widetilde{I}_f^2} &= \frac{I_f}{\theta_f^*(x_f)}\left[1-\frac{I_f}{\theta_f^*(x_f)^2}\frac{1}{x_f(1-x_f)}\right]. \end{aligned}$$

Define $h(x_f) := x_f(1-x_f)\theta_f^*(x_f)^2 - I_f$. If $h(x_f) > 0$, then $x_f(\widetilde{I}_f)$ is (strictly) convex. Note that $h'(x_f) = (1-2x_f)\theta_f^*(x_f)^2 + \theta_f^*(x_f) > 0$, which implies $h(x_f)$ is increasing with x_f, and hence, for $x_f \in (\beta_f, 0.5)$, $h(x_f) > h(\beta_f) = 0$.

Define $g(x,y) = e^{x+y}$. consider the function

$$\begin{aligned} f(x,y) &= \ln(1-e^{-D_f g(x,y)}) \\ \frac{\partial f}{\partial x} &= \frac{D_f e^{-D_f g}}{1-e^{-D_f g}}\frac{\partial g}{\partial x} \\ \frac{\partial f}{\partial x} &= \frac{D_f g e^{-D_f g}}{1-e^{-D_f g}}. \end{aligned}$$

Similarly

$$\frac{\partial f}{\partial y} = \frac{D_f g e^{-D_f g}}{1-e^{-D_f g}}.$$

Also

$$\begin{aligned} \frac{\partial^2 f}{\partial x\partial y} &= \frac{-D_f^2 g^2 e^{-2D_f g}}{(1-e^{-D_f g})^2} + \frac{D_f g e^{-D_f g}}{1-e^{-D_f g}} - \frac{-D_f^2 g^2 e^{-D_f g}}{1-e^{-D_f g}} \\ &= \frac{-D_f g}{(1-e^{-D_f g})^2}\cdot\big[D_f g e^{-2D_f g} + \\ &\quad D_f g(1-e^{-D_f g})e^{-D_f g} - (1-e^{-D_f g})e^{-D_f g}\big] \\ &= \frac{-D_f g}{(1-e^{-D_f g})^2}\left[D_f g - (1-e^{-D_f g})e^{-D_f g}\right]. \end{aligned}$$

Similarly, one can show that $\frac{\partial^2 f}{\partial x^2} = \frac{\partial^2 f}{\partial y^2} = \frac{\partial^2 f}{\partial x\partial y}$. Define $\ell(x) = D_f x - (1-e^{-D_f x})e^{-D_f x}$. If $\ell(x) > 0$, then $f(x,y)$ is (strictly) convex. Note that $\ell'(x) = (D_f - D_f e^{-2D_f x}) + (D_f e^{-D_f x} - D_f e^{-2D_f x}) > 0$. Therefore, $\ell(x) > \ell(0) = 0$. ■

Appendix E
Proof of Lemma 5

From (21), it is clear that even for a single cell, because of the nonzero second term in the LHS, the airtime of flow f given by $\frac{n_f}{w_{f,c}}$ is not the same for all the flows f. ■

References

[1] R. Li and A. Eryilmaz, "Scheduling for end-to-end deadline-constrained traffic with reliability requirements in multi-hop networks," in *Proc. IEEE INFOCOM*, Shanghai, China, Apr. 2011, pp. 3065–3073.

[2] J. Jaramillo and R. Srikant, "Optimal scheduling for fair resource allocation in ad hoc networks with elastic and inelastic traffic," *IEEE/ACM Trans. Netw.*, vol. 19, no. 4, pp. 1125–1136, Aug. 2011.

[3] A. Checco and D. J. Leith, "Proportional fairness in 802.11 wireless LANs," *IEEE Commun. Lett.*, vol. 15, no. 8, pp. 807–809, Aug. 2011.

[4] X. Chen and D. J. Leith, "Frames in outdoor 802.11 WLANs provide a hybrid binary symmetric/packet erasure channel," 2012 [Online]. Available: http://arxiv.org/abs/1209.4504

[5] M. Chiang, S. H. Low, A. R. Calderbank, and J. C. Doyle, "Layering as optimization decomposition: A mathematical theory of network architectures," *Proc. IEEE*, vol. 95, no. 1, pp. 255–312, Jan. 2007.

[6] L. Georgiadis, M. Neely, and L. Tassiulas, *Resource Allocation and Cross-Layer Control in Wireless Networks*. Boston, MA, USA: Now, 2006.

[7] S. Shakkottai and R. Srikant, *Network Optimization and Control*. Boston, MA, USA: Now, 2008.

[8] K. Premkumar, X. Chen, and D. J. Leith, "Utility optimal coding for packet transmission over wireless networks—Part I: Networks of binary synchronous channels," in *Proc. 49th Annu. Allerton Conf. Commun., Control, Comput.*, Monticello, IL, USA, Sep. 2011, pp. 1592–1599.

[9] F. J. MacWilliams and N. J. A. Sloane, *The Theory of Error-Correcting Codes*. Amsterdam, The Netherlands: North-Holland, 1977.

[10] R. Smarandache, H. Gluesing-Luerssen, and J. Rosenthal, "Constructions of MDS-convolutional codes," *IEEE Trans. Inf. Theory*, vol. 47, no. 5, pp. 2045–2049, Jul. 2001.
[11] D. P. Bertsekas, A. Nedich, and A. E. Ozdaglar, *Convex Analysis and Optimization*. Belmont, MA, USA: Athena Scientific, 2003.

Karumbu Premkumar (M'13) received the Ph.D. degree in engineering from the Indian Institute of Science, Bangalore, India, in 2011.

From 2010 to 2012, he was a Post-Doctoral Research Fellow with the Hamilton Institute, National University of Ireland Maynooth, Maynooth, Ireland. Since 2012, he has been an Associate Professor with the SSN College of Engineering, Chennai, India. His research interests are in resource allocation, performance modeling, analysis, design, and optimization problems arising in communication networks.

Xiaomin Chen received the M.Sc. degree from Beijing University of Posts and Telecommunications, Beijing, China, in 2008, and the Ph.D. degree from the Hamilton Institute, NUI Maynooth, Maynooth, Ireland, in 2012, both in engineering.

She is currently a Postdoctoral Research Fellow with the Hamilton Institute, NUI Maynooth. Her research interests lie in coding, protocol design, and resource allocation in wireless networks.

Douglas J. Leith (M'02–SM'09) graduated from the University of Glasgow, Glasgow, U.K., in 1986, where he received the Ph.D. degree in engineering in 1989.

In 2001, he moved to the National University of Ireland, Maynooth, Ireland, to assume the position of SFI Principal Investigator and to establish the Hamilton Institute (http://www.hamilton.ie), of which he is Director. His current research interests include the analysis and design of network congestion control and resource allocation in wireless networks.